Martínez-Haya, R.; Sabater Marco, C.; Castillo López, M.; Miranda Alonso, MÁ.; Marín García, ML. (06-2). A mechanistic study on the potential of quinolinium salts as photocatalysts for the abatement of chlorinated pollutants. Journal of Hazardous Materials. 351:277-284. https://doi.org/10.1016/j.jhazmat.2018.03.010

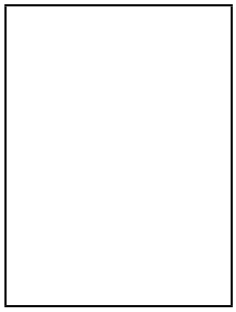

Title: A Mechanistic Study on the Potential of Quinolinium Salts as Photocatalysts for the Abatement of Chlorinated Pollutants

Authors: Rebeca Martinez-Haya, Consuelo Sabater, Maria-Ángeles Castillo, Miguel A. Miranda, M. Luisa Marin

A Mechanistic Study on the Potential of Quinolinium Salts as Photocatalysts for the Abatement of Chlorinated Pollutants

Rebeca Martinez-Haya,[a] Consuelo Sabater,[b] Maria-Ángeles Castillo,[b] Miguel A. Miranda[a,*] and M. Luisa Marin[a,*]

[a]Instituto de Tecnología Química, Universitat Politècnica de València-Consejo Superior de Investigaciones Científicas, Avda. de los Naranjos s/n, E-46022, Valencia, Spain

[b]Departamento de Biotecnología, Universitat Politècnica de València, Camino de Vera s/n, E-46022 Valencia, Spain

*Corresponding author

E-mail addresses: marmarin@qim.upv.es; mmiranda@qim.upv.es

GRAPHICAL ABSTRACT

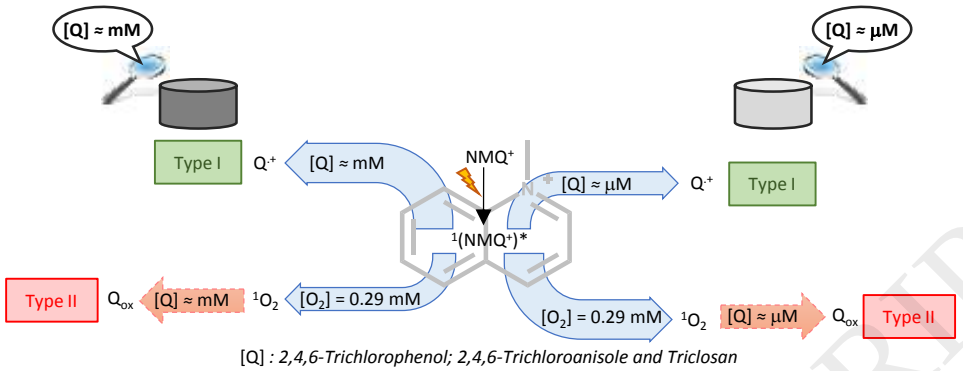

HIGHLIGHTS

- Degradation of chlorinated pollutants is achieved using NMQ^+ as photocatalyst
- Pollutants quench singlet excited state of NMQ^+ with 10^9 $M^{-1}s^{-1}$ rate constants
- Laser flash photolysis shows formation of $NMQ^{\bullet}$, a fingerprint of the redox processes
- Pollutants quench singlet oxygen with typical 10^5-10^6 $M^{-1}s^{-1}$ rate constants
- Kinetic analysis of the competitive pathways indicates mainly Type I photodegradation

Abstract

Photocatalytic degradation of three highly chlorinated contaminants, namely 2,4,6-trichlorophenol (TCP), 2,4,6-trichloroanisole (TCA) and 5-chloro-2-(2,4-dichlorophenoxy)phenol (triclosan, TCS) has been investigated in the presence of *N*-methylquinolinium tetrafluoroborate (NMQ^+), a photocatalyst able to act *via* Type I or Type II mechanism. Photodegradation of contaminants under aerobic conditions was achieved within hours; and it was accompanied by mineralization, as demonstrated by trapping of the evolved carbon dioxide as barium carbonate. Moreover, a high degree of detoxification, based on % inmobilization of daphnids (*Daphnia magna* bioassay), was

reached after 70 hours of irradiation. Quenching of the NMQ^+ fluorescence by the pollutants was evidenced by a decrease in the emission intensity and lifetime. Detection of the reduced $NMQ^{\bullet}$ by laser flash photolysis in the presence of the pollutants provided an unambigous evidence of the electron transfer process. Quenching of singlet oxygen by the contaminants showed the typical singlet oxygen quenching constants (10^5-10^6 $M^{-1}s^{-1}$). Evaluation of the relative contribution of both pathways (Type I vs Type II) point to the photodegradation occurring *via* a Type I mechanism, being the contribution of Type II mechanism negligible at any concentration range.

Keywords

Electron transfer; laser flash photolysis; singlet excited state; singlet oxygen; time-resolved fluorescence

1. Introduction

Development of civilizations is associated with availability of high quality water resources. [1] However, the need for pesticides to ensure nourishment of mankind together with the huge consumption of drugs and personal care chemicals contribute to increase the volume of wastewater effluents that need to be treated to guaranty the required standards for drinking water.[2, 3] Particular attention deserves the variety of chlorinated hydrocarbons that have been identified as persistent toxins in the environment and also as a serious threat to human health.[4]

Photocatalysis constitutes an emerging green process that can be applied, among others, to water remediation.[5, 6] In this sense, advanced oxidation processes, such as those able to generate hydroxyl radicals (photo-Fenton or TiO_2)[7-14] have demonstrated to be efficient methodologies to eliminate contaminants from aqueous systems.[6, 15, 16] Moreover, the use of organic photocatalysts offers the possibility of investigating the reaction mechanisms upon studying the kinetics of their different excited states in the presence of the selected pollutants based on time-resolved techniques in the nano or micro-second scale.[17] For instance, triphenyl(thia)pyrylium salts are widely used examples of photocatalysts acting *via* electron transfer (Type I) from their singlet or triplet excited states. In fact, we have recently demonstrated the involvement of the singlet excited state of triphenylthiapyrylium salts in the photodegradation of dimethoate, alachlor and pyrimethanil[18] or the participation of the triplet excited state of triphenylpyrylium salts in the removal of 2,6-dichlorodiphenylamine-based drugs.[19] In addition, participation of singlet oxygen in the photodegradation of contaminants (Type II) when using Rose Bengal or Methylene Blue among others, has also been extensively reported in literature.[20, 21]

Herein, we are focusing our attention in a different organic photocatalyst, namely *N*-methylquinolinium (NMQ^+) tetrafluoroborate, due to its singular photophysical properties. Its singlet excited state is quite energetic (E_S = 341 kJ mol^{-1}), long-lived (20 ns) and exhibits emission centered at 402 nm with a high quantum yield (Φ_F = 0.85).[17] In addition, due to the energy gap between the first singlet and triplet excited states ($\Delta E \approx 86$ kJ mol^{-1}), singlet oxygen is efficiently generated from its singlet excited state and thus, the overall yield is Φ_Δ = 0.85.[17] Furthermore, the reported redox potential for

NMQ^+ is E_{red} = -0.85 V *vs* SCE);[22] thus, formation of superoxide anion from molecular O_2 (E_{red} = -0.33 V *vs* SCE) and reduced $NMQ^{\bullet}$ is exergonic.[23]

Moreover, in the cases of cationic photocatalysts as NMQ^+, photoinduced electron transfer (PET) is usually very efficient due to the lack of Coulombic attraction between the resulting species; therefore, back-electron transfer (BET), that is usually the main side process, is unlikely. All these reasons convert NMQ^+ tetrafluoroborate into a photocatalyst that could, in principle, promote photodegradation of pollutants through Type I (electron transfer) and/or Type II (singlet oxygen formation) mechanisms. Based on these characteristics, various examples of oxidation of aromatic sulfides and sulfoxides from $^1(NMQ^+)^*$ have already been described.[24-30] The main drawback of NMQ^+ tetrafluoroborate could be attributed to the fact that it is not commercially available although it can be straightforward synthesized upon methylation of quinoline.[22, 31] Moreover, its UV absorption extends only up to 380 nm; thus it employs a small part of the solar spectrum and could be considered of limited use. Nevertheless, its stability and the possibility of analysing the contribution of Type I *versus* Type II oxidation, both happening from the singlet excited state, makes this photocatalyst very interesting from the mechanistic point of view, and the obtained results could be extrapolated to others, that would extend their absorption into the visible range.[27]

With this background, the main goal of the present paper is to investigate on the role of the competitive mechanisms that, in principle, could be acting when using NMQ^+ as a representative photocatalyst of the quinolinium salts family (Type I *vs* Type II). To illustrate this concept, three chlorinated pollutants have been selected, namely 2,4,6-trichlorophenol (TCP), 2,4,6-trichloroanisole (TCA) and 5-chloro-2-(2,4-dichlorophenoxy)phenol (triclosan, TCS) (Fig. 1). TCP can be found together with other chlorophenols in drinking water as a consequence of chlorination of phenols;[32] TCA is a typical pollutant of the dark complex liquor resulting from the wastewaters of cork industry[33] and TCS is a common antibacterial agent in personal care products that is incompletely removed in conventional wastewater treatment plants; thus TCS concentrations of 0.24-37.8 μg/L have been detected in treated effluents.[34] Photodegradation of these pollutants upon irradiation in the presence of NMQ^+ will be evaluated and time-resolved photophysical techniques will help understanding the main operating mechanisms.

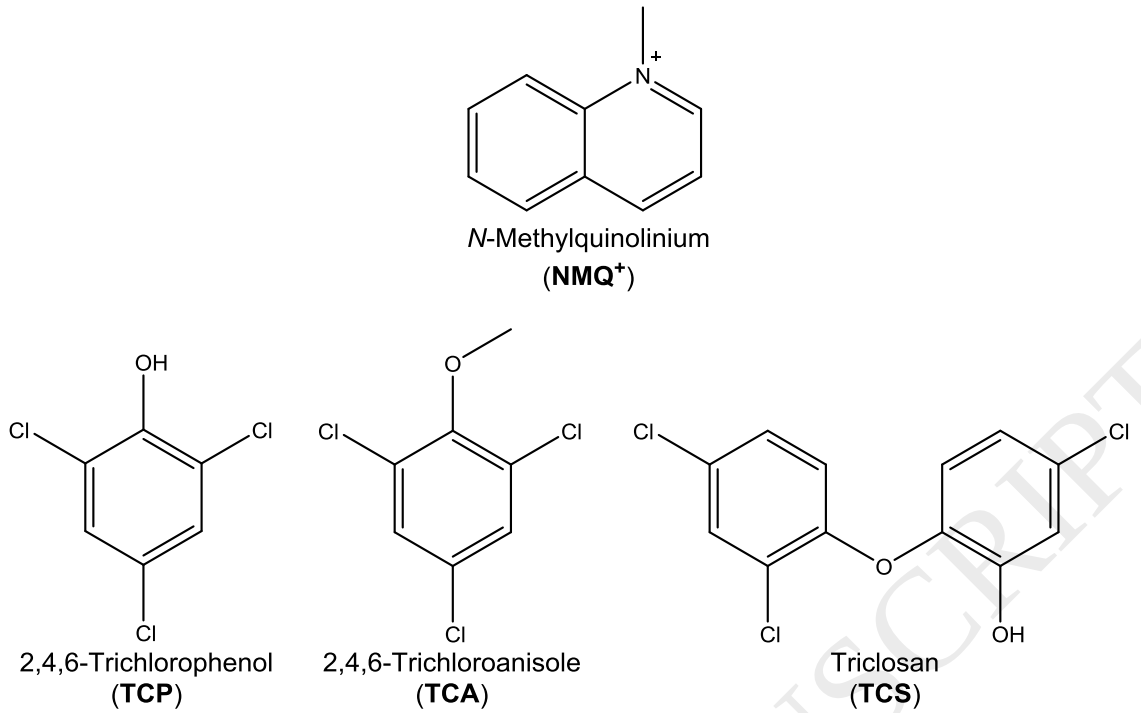

Figure 1

2. Experimental

2.1. Chemicals

N-methylquinolinium tetrafluoroborate salt was obtained from quinoline (Aldrich) in two steps as described previously.[22, 31, 35] Thus, quinoline (0.42 mol) and methyl iodide (0.64 mol, 1.5 eq) were heated in a round bottom flask, at 65 ºC, under reflux for 24 hours, and the resulting solid (*N*-methylquinolinium iodide) was washed with ether. ^{1}H (300 MHz, CD_3OD): δ (ppm) 4.72 (s, 3H, CH_3); 8.09 (m, 2H); 8.31 (m, 1H); 8.45 (d, *J* = 8.3 Hz, 1H); 8.53 (d, *J* = 9.1 Hz, 1H); 9.23 (d, *J* = 8.4 Hz, 1H); 9.40 (d, *J* = 5.9 Hz, 1H); ^{13}C NMR (75 MHz, CD_3OD): δ (ppm) 46.3, 119.8, 123.0, 131.3, 131.5, 131.8, 137.2, 140.4, 148.9, 151.1. The crude *N*-methylquinolinium iodide was treated with $BF_3{\cdot}Et_2O$ (2.6 eq) under nitrogen atmosphere. The mixture was stirred and heated at 50ºC under reflux for 2.5 hours. An additional amount of $BF_3{\cdot}Et_2O$ was then added and the mixture was stirred for another 2.5 hours. The resulting solid was washed with ether and recrystallized from ethanol to yield *N*-methylquinolinium tetrafluoroborate. ^{1}H (300 MHz, CD_3OD): δ (ppm) 4.70 (s, 3H, CH_3); 8.06 (m, 2H); 8.29 (m, 1H); 8.42 (d, *J* = 8.2 Hz, 1H); 8.51 (d, *J* = 9.0 Hz, 1H); 9.19 (d, *J* = 8.5 Hz, 1H); 9.33 (d, *J* = 5.6 Hz, 1H); ^{13}C NMR (75 MHz, CD_3OD): δ (ppm) 46.2, 119.8, 122.9, 131.3, 131.4, 131.7, 137.2, 140.3, 148.8, 151.1.

N-methylquinolinium tetrafluoroborate was adsorbed onto Y zeolite 100 according to a procedure described previously for other organic photocatalysts. [36] Briefly, Y-zeolite 100 (6.2 g) was suspended in 25 mL of an aqueous solution containing *N*-methylquinolinium tetrafluoroborate (1.0 g). The mixture was heated at 40ºC and stirred for 24 hours in the dark. Then, the solid was filtered, washed with water (30 mL) and dried at 100ºC for 72 hours. Elemental analysis indicated a loading of NMQ^+ on zeolite Y of 13.8% wt.

1,4-Diazabicyclo[2.2.2]octane (DABCO), 2,4,6-trichlorophenol (TCP), 2,4,6-trichloroanisole (TCA), triclosan (TCS), barium hydroxide octahydrate, 2-nitrobenzoic acid and TiO_2, as AEROXIDE® P25-TiO_2, were obtained from Aldrich. Zeolite Y 100 was obtained from Zeolyst International. Water used in photodegradation experiments was Milli-Q grade, acetonitrile (ACN) and ethanol were of HPLC quality from Merck.

2.2. Photodegradation

Homogeneous photochemical reactions were performed in test tubes with magnetic stirring using a Luzchem photoreactor (model LZC-4 V) equipped with 12 lamps emitting at 350 nm. Aqueous solutions of 10 mL containing TCP, TCA or TCS (3×10^{-5} M) and NMQ^+ (3×10^{-7} M) were irradiated under air. In all cases, the pH of the solutions remained stable along irradiation time. The removal of the pollutants was monitored by HPLC at different irradiation times. Thus, 5 μL of 2-nitrobenzoic acid (8.8×10^{-4} M) were added as internal standard to every aliquot (75 μL) before injection. The HPLC was an Agilent 1100 Series model with quaternary pump G1311A, photodiode detector DAD G1315B, standard liquid autosampler G1313A and degasser G1322A. A Mediterranea Sea 18 column (25 mm × 0.46 mm, 5 μm particle size) was employed. The mobile phase was fixed at 1.5 mL min^{-1} with an isocratic mixture of water pH 3 (20%) and acetonitrile (80%). In order to monitor removal of the pollutants, the detection wavelength was fixed at 215 nm for TCP, TCA and TCS.

The mineralization was tested upon *in situ* trapping the formed carbon dioxide as $BaCO_3$. For that purpose, an aqueous solution (40 mL) of a mixture of the three pollutants (2 g L^{-1} each) and NMQ^+ (30 mg L^{-1}) was irradiated on a solar simulator for 48 hours upon stirring, and under a continuous flow of oxygen. The evolved CO_2 was *in situ* trapped as $BaCO_3$ by bubbling it through a saturated solution of $Ba(OH)_2$. The resulting precipitate was submitted to elemental analysis using a EuroEA Elemental Analyser from

EuroVector Instruments and Software. The analysis qualitatively confirmed the nature of the new precipitate as $BaCO_3$.

For the heterogeneous photoreactions, aqueous solutions of 10 mL containing a mixture of one of the pollutants (3 x 10^{-4} M each) and supported Zeolite Y-NMQ^+ (70 mg L^{-1}) were irradiated under air, using the above described Luzchem photoreactor. The removal of the pollutants was monitored by HPLC at different irradiation times.

For the toxicity assays, aqueous solutions of 250 mL containing the mixture of the three pollutants (3 x 10^{-5} M each), and either NMQ^+ (10 mg L^{-1}, photomixture A) or TiO_2 (200 mg L^{-1}, photomixture B) were irradiated using the above described Luzchem photoreactor under aerobic atmosphere, up to 70 hours.

2.3. Photophysical instrumentation

A Shimadzu UV-2101PC spectrophotometer was employed to perform the UV/Vis absorption spectra.

Steady-state and time-resolved fluorescence experiments were carried out on a Photon Technology International (PTI) LPS-220B spectrofluorometer and on a EasyLife V spectrofluorometer from OBB, respectively. In the case of time-resolved fluorescence, the apparatus was equipped with a pulsed LED (λ_{exc} = 310 nm) excitation source; residual excitation signal was filtered in emission by using a cut-off filter (50% transmission at 320 nm). Monoexponential decay functions that use a deconvolution procedure to separate them from the lamp pulse profile provided the fitted kinetic traces.

A pulsed Nd: YAG SL404G-10 Spectron Laser Systems at the excitation wavelength of 355 nm was employed to carry out the laser flash photolysis (LFP) experiments. The energy of the single pulses (~10 ns duration) was lower than 15 mJ $pulse^{-1}$. The laser flash photolysis system is formed by the pulsed laser, a pulsed Lo255 Oriel Xenon lamp, a 77200 Oriel monochromator, an Oriel photomultiplier tube (PMT) housing, a 70705 PMT power supply and a TDS-640A Tektronix oscilloscope. Lifetime of singlet oxygen was recorded at 1270 nm with a Hamamatsu NIR detector upon excitation with a 355 nm Nd:YAG laser.

Photophysical measurements in solution were run at room temperature under nitrogen using quartz cells of 1 cm optical path length. For the fluorescence experiments, deaerated

acetonitrile solutions of NMQ^+ (absorbance lower than 0.15 at λ_{exc} = 317 nm) were treated with increasing concentrations of pollutant (up to 5 x 10^{-3} M). Transient absorption spectra were obtained from a deaerated solution of NMQ^+ in acetonitrile (absorbance lower than 0.3 at λ_{exc} = 355 nm) containing TCP, TCA or TCS (3 x 10^{-3} M).

Diffuse reflectance of supported Zeolite Y-NMQ^+ was recorded using a Cary 5000 from Agilent Technologies. Solid emission fluorescence of supported Zeolite Y-NMQ^+ was recorded upon excitation at λ_{exc} = 317 nm, and collected at 90º to minimize the scattered light.

2.4. Toxicity assays

Ephippia (dormant eggs) of crustacean *Daphnia magna* (*D. magna*) were supplied by ECOtest S.L. (Valencia, Spain). Bioassays based on the inhibition of the mobility of *D. magna* were performed according to the standard ISO 6341:1996 procedure,[37] which uses 24-h old organisms hatched from the ephippia. Five neonates were placed in appropriate containers with 10 mL of different dilutions of photomixtures A or B, or with 10 mL of aqueous solutions of their components separately. The assays were conducted in a climate chamber in the dark at a constant temperature of 21 ± 1 ºC. At the end of the test period (24 h) mobile *D. magna* were counted in each container. Those unable to swim in the 15 s after agitation were considered immobile. Sample dilutions and controls were prepared with the standard freshwater (11.76 g L^{-1} $CaCl_2 \cdot 2H_2O$; 4.93 g L^{-1} $MgSO_4 \cdot 7H_2O$; 2.59 g L^{-1} $NaHCO_3$; 0.23 g L^{-1} KCl); all of them were tested in quadruplicate. Standard freshwater was also used as hatching medium. Water quality parameters such as pH, temperature, and dissolved oxygen were measured in the test media before and after the 24 h exposure. The test solution was not replaced in this 24 h static non-renewal test. Before the acute test, daphnia neonates were fed for 2 h with freshwater algae.

Whenever possible, assay data were used to calculate the EC_{50} (concentration required to produce 50% of effect) by Probit analysis, using the Statistical Analysis System SPSS (version 16.0). Toxicity data were statistically analyzed to determine the effect of irradiation procedure on toxicity. A $p < 0.05$ was taken to indicate statistical significance (STATGRAPHICS PLUS version 5.1).

3. Results and Discussion

3.1. Photochemical degradation

Homogeneous aqueous solutions containing TCP, TCA or TCS were irradiated in the presence of NMQ^+ (1% mol), with 350 nm centred light, under aerated atmosphere. The evolution of the relative concentration of each pollutant with irradiation time is shown in Fig. 2. In the case of TCP and TCA photodegradation was complete in 25 hours, while TCS was more reluctant and only 70% degradation was observed in this case at the same irradiation time. No additional clear peaks were found in the HPLC analysis, indicating that under the employed conditions the starting pollutants disappear giving rise probably to several photoproducts, and therefore their concentration is not enough to be detected. Comparison of the UV-visible spectra of NMQ^+ and the three pollutants indicates that the photocatalyst is the only species capable of absorbing 350 nm-light (see Fig. S1). Control experiments carried out in the absence of photocatalyst or light showed that the three pollutants remained stable after equivalent reaction periods (see Fig. S2 and S3); NMQ^+ was also stable when subjected to irradiation in the absence of the pollutants (see Fig. S4). A further control was carried out to investigate on the participation of oxygen in the photodegradation. For this purpose, two parallel sets of experiments were set-up: homogeneous aqueous solutions containing TCP, TCA or TCS were irradiated in the presence of NMQ^+, under deaerated/aerated atmospheres (see Fig. S5). In order to reduce irradiation times, higher amount of NMQ^+ was used (10 mg/L). In fact, removal of contaminants was independent on the presence of air, or for the case of TCS even faster in the absence of oxygen, pointing to a more effective photodegradation starting *via* electron transfer mechanism.

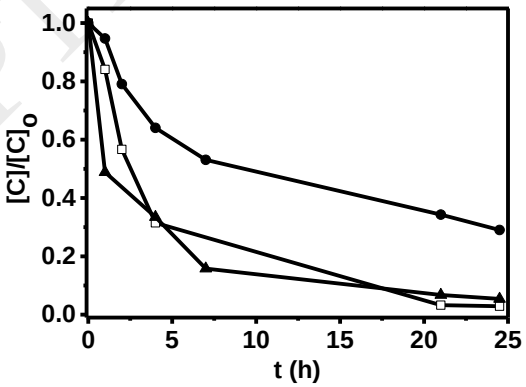

Figure 2

To check whether mineralization could be occurring under aerobic conditions as the overall result of photodegradation, the possible formation of CO_2 was investigated. For this purpose, a new batch containing the mixture of the three contaminants and NMQ^+

was irradiated in the solar simulator upon continuous flow of oxygen. The CO_2 obtained upon mineralization was bubbled through a saturated aqueous solution of $Ba(OH)_2$, producing $BaCO_3$ that precipitated at the bottom. After 48 hours irradiation, the precipitate was filtered and submitted to elemental analysis, which unequivocally confirmed the formation of $BaCO_3$, although quantification was not considered necessary at that stage.

At this point, the performance of NMQ^+ as homogeneous photocatalyst had already been demonstrated. Beyond that, to improve the potential applicability of the system, further experiments, such as heterogeneization, as a preliminary step for future scale-up, was investigated. For this purpose, NMQ^+ was supported onto an inert inorganic support (zeolite Y 100), elemental analysis showed a loading of *ca*. 13 % NMQ^+ weight, diffuse reflectance and emission (see Figure S6A and S6B, respectively) unequivocally demonstrated the incorporation of the photocatalyst onto the support. To evaluate the performance of Zeolite Y-NMQ^+ on the heterogeneous photodegradation of the pollutants, aqueous mixtures of each pollutant (3×10^{-4} M) and the supported Zeolite Y-NMQ^+ (70 mg L^{-1}) were separately irradiated with 350 nm centered light, under aerated atmosphere. The removal of the pollutants versus time under heterogeneous conditions is shown in Fig. 3.

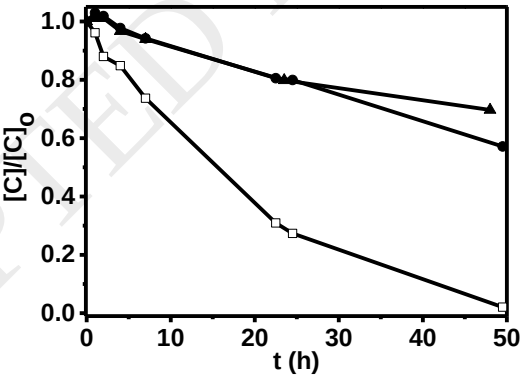

Figure 3

As it can be seen in Figure 3, heterogeneous photodegradation of TCP, TCA and TCS led to efficient degradation of the three pollutants; although reaction times were longer than under homogeneous conditions. It has to be taken into account that the concentrations were one order of magnitude higher. Control experiments indicated that removal of the pollutants upon adsorption on the Zeolite Y-NMQ^+ was lower than 10%, so the photodegradation could safely be attributed to the photocatalyzed oxidation.

3.2. Toxicity evaluation

Even more important than to complete a mechanistic study on the photodegradation of these chlorinated compounds was to assess whether detoxification was taking place and therefore to evaluate the potential of an advanced oxidation process based on the use of organic photocatalysts such as NMQ^+ to be eventually applied to real wastewaters. For this purpose, biological assays were carried out using *D. magna* as the model system.[38, 39] A set of two parallel experiments were conducted in which mixtures of the three pollutants were irradiated in the presence of either NMQ^+ (photomixture A) or the benchmark photocatalyst P25-TiO_2 (photomixture B). Table 1 lists the results of the initial toxicity test for each of the compounds used in the photoirradiations expressed as EC_{50} values with their 95% confidence intervals. The results indicate that initially NMQ^+ exhibits a similar level of toxicity than TCP, TCA or TCS. Nevertheless, since NMQ^+ was used as 1% mol its toxicity was estimated negligible. Although DMSO is considered to be non toxic, it was also included in the bioassay since it was used to predissolve the contaminants. Next, the toxicity results obtained upon 70 hours irradiation, for the photomixtures A and B are shown on Fig. 4 top and bottom, respectively. Irradiated (light bars) and non-irradiated control experiments (dark bars) are shown together for a better comparison. Results are expressed as % of inmobilization of daphnids at serial dilutions of aqueous solutions. The initial toxicity values of the two photomixtures decreased along irradiation, achieving for the case of NMQ^+ (photomixture A, Fig. 4 top) a higher degree of detoxification as compared with TiO_2 samples (photomixture B, Fig. 4 bottom).

Table 1

Sample	EC_{50} *(Daphnia magna)*
DMSO[a]	5.3 (4.2 - 7.8) 10^{-2} M
NMQ	2.0 (1.4 - 3.1) 10^{-5} M
TiO_2	-[a]
TCP	[0.9 (0.6 - 1.4)] 10^{-5} M
TCA	[1.7 (1.5 - 1.9)]·10^{-5} M
TCS	[0.5 (0.4 - 0.6)] 10^{-5} M

[a] maximum toxicity sample < 40%

At 1:1 dilution and even at 1:2, the non-irradiated samples (dark bars) exhibited a high toxicity (100% immobilization), which decreased progressively with irradiation time. After 70 hours of irradiation, the photomixture A exhibited a significant decrease in the toxicity level even at 1:1 dilution (see light bars compared to dark ones in Fig 4 top). That pronounced detoxification was more clearly observed in all cases upon dilution. At the final irradiation time the photomixture treated with NMQ^+ exhibited a lower toxicity than the photomixture treated with TiO_2 (compare light bars in Fig 4, top *versus* bottom), thus proving that the use of organic photocatalysts could have a beneficial effect not only on the degradation of pollutants but also on the detoxification of treated wastewaters.

Althouhg TiO_2 solution show remarkably less toxicity than NMQ^+, the presence of TiO_2 enhanced the toxicity of the photomixture B up to 1:8 dilution. Previous ecotoxicity studies on model aquatic organisms reported the great variability in the toxicity level of TiO_2 particles, with EC_{50} values that ranged from 1.62 mg L^{-1} to over 100 mg L^{-1}, in assays conducted with several species of *Daphnia*.[40-42] Moreover, Fan *et al.* demonstrated that, at a safe environmental concentration of Cu, TiO_2 particles notably increased the toxicity of the metal on *D. magna*.[43]

The higher toxicity values found in the photomixture B could be due to the observed aggregation of particles that could act as a trap for neonates of *Daphnia,* eventually causing death. The main toxicity mechanism of action reported for TiO_2 is oxidative stress,[44, 45] resulting in cell damage, genotoxicity, inflammation, immune response, etc.[46] Although additional effects related with the physical and chemical characteristics of TiO_2 have also been reported, such as the aggregation of particles that involves modifications in bioavailability and reactivity of other present substances or variations in biological behaviour of the exposed organisms.[47-49]

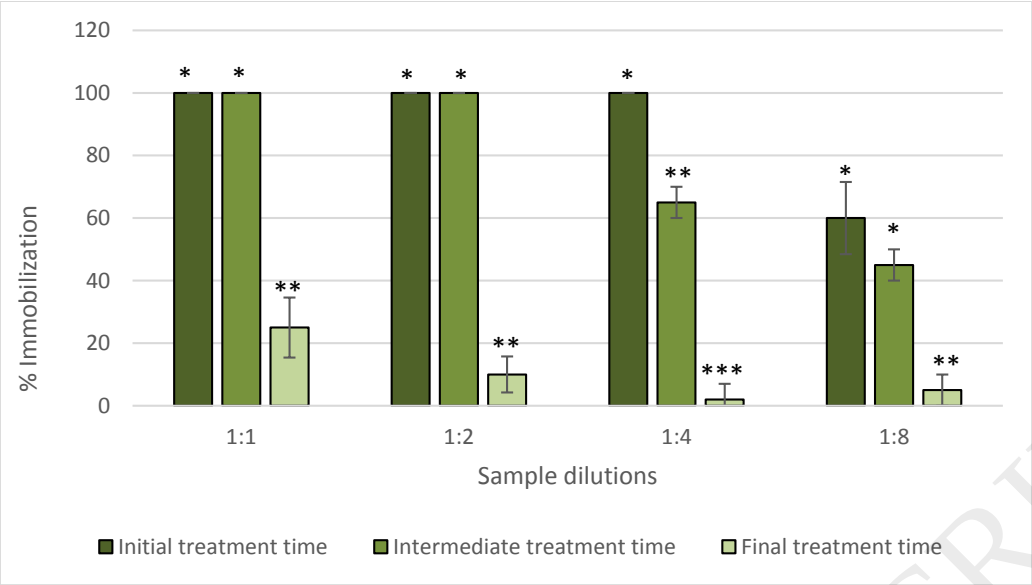

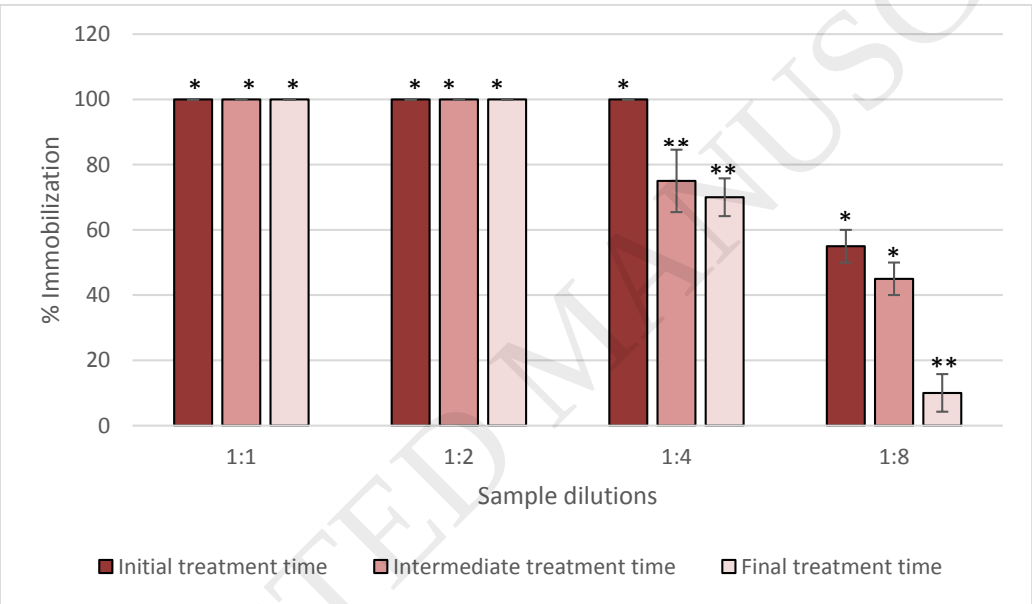

Figure 4

3.3. Photophysical studies

Redox potential of NMQ^+ from its singlet excited state is very high (*ca.* 2.7 V), which means that, upon excitation, this photocatalyst becomes a highly oxidizing species. Moreover, singlet oxygen is obtained with high yield (Φ_Δ *ca.* 0.85).[22] Nevertheless, the kinetic viability of the processes or, even more, the contribution of each acting pathway when more than one is thermodynamically feasible, has to be determined from a kinetic-based rationale, based on fast-kinetic techniques. In this context, time-resolved fluorescence (in the nanosecond time scale) and Laser Flash Photolysis (LFP) (in the

microsecond scale with absorption or emission detection) cover the timescales of particularly important physical and chemical processes, including those generated from photoinduced electron transfer (Type I) or singlet oxygen reactivity (Type II). Therefore, rate constants for the PET were obtained from the quenching experiments of NMQ^+ singlet excited state by the contaminants using time-resolved fluorescence. Analogously, rate constants for the reactivity of singlet oxygen with the pollutants were determined using LFP with time-resolved emission detection. When singlet oxygen is independently generated its behaviour in the presence of the contaminants is cleanly analysed. Finally, the relative contribution of both pathways is evaluated to understand the role of every species in the photodegradation processes.

3.3.1. Emision quenching studies

Steady-state and time-resolved experiments were carried out to evaluate the extent of the electron transfer oxidation from the singlet excited state of NMQ^+. In fact, the fluorescence emission intensity and also the singlet lifetime decreased upon addition of increasing amounts of each pollutant in deaerated acetonitrile. The corresponding quenching rate constants were determined by means of the Stern-Volmer equation plotting I_0/I and τ_0/τ *versus* pollutant concentration (see Fig. 5).

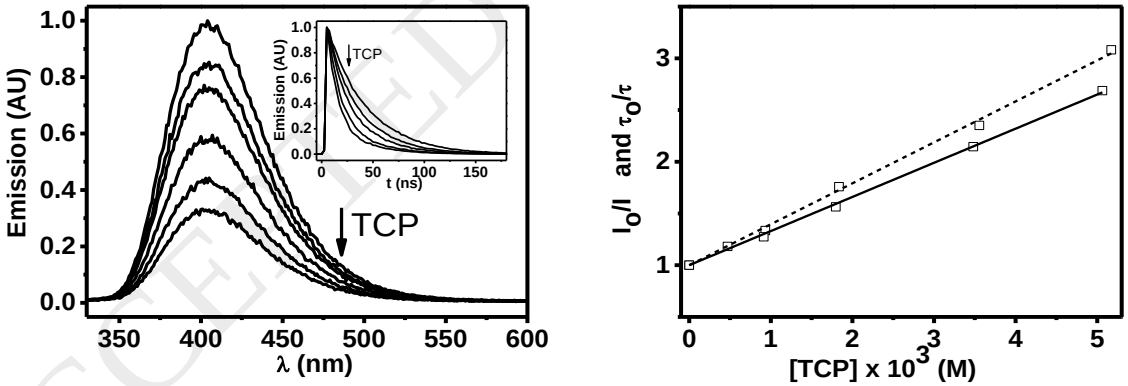

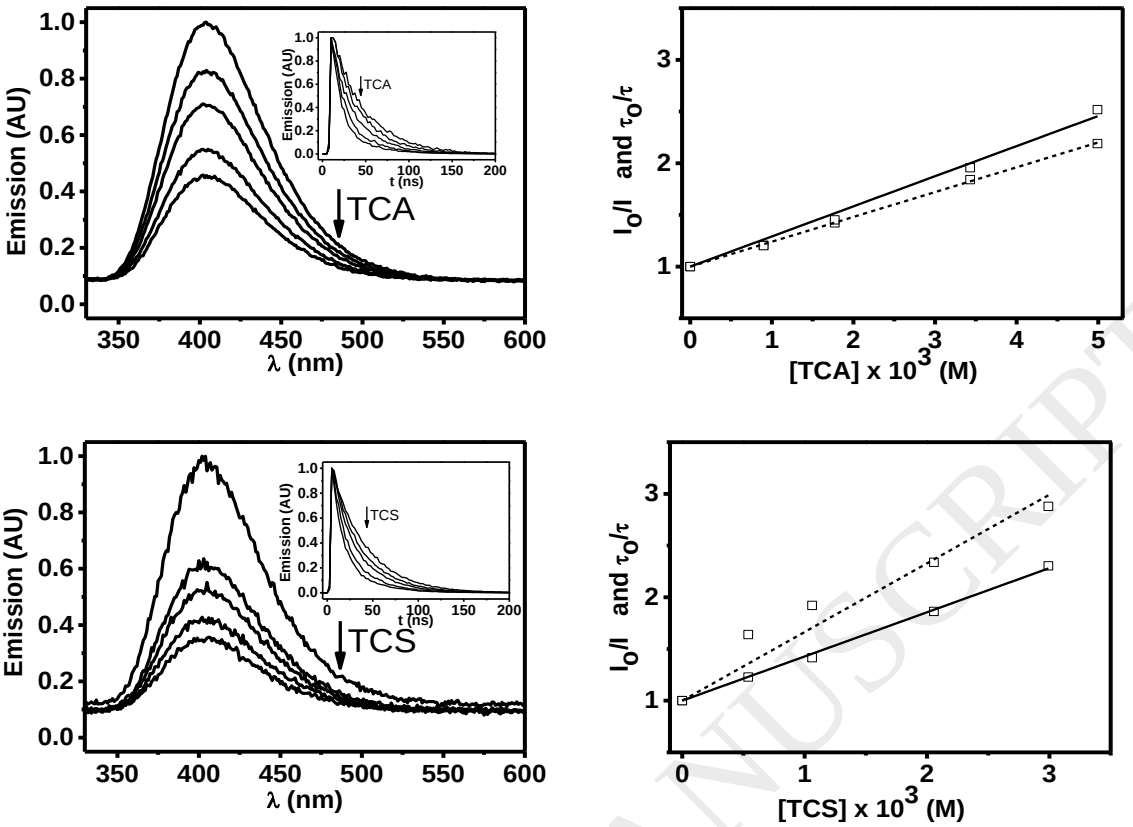

Figure 5

The dynamic nature of the electron transfer process was supported by the decrease in the lifetime of NMQ^+; the corresonding rate constant values are shown on Table 2. The rate constant values obtained for the static and dynamic quenching of the singlet excited state of NMQ^+ by oxygen are also included (see also Fig. S7). They were in all cases close to the diffusion limit in CH_3CN (k_{diff} = 1.9 x 10^{10} $M^{-1}s^{-1}$).[50]

Next, the possible participation of $^1O_2$ was evaluated by recording the lifetime of its characteristic emission band at 1270 nm upon increasing concentration of the pollutants (see Stern-Volmer plots in Fig. S8). In all cases, $^1O_2$ was poorly quenched by the pollutants with k_{q1O2} between 5.3 x 10^5 $M^{-1}s^{-1}$ and 1.3 x 10^6 $M^{-1}s^{-1}$ (Table 2). These values, although comparatively low, are in the range of the typical values for $^1O_2$ quenching by organic compounds.[51]

Table 2

Quencher	k_{qS} x 10^{-9}, $M^{-1}s^{-1}$ (from steady-state experiments)	k_{qS} x 10^{-9}, $M^{-1}s^{-1}$ (from time-resolved experiments)	$k_{q^1O_2}$ x 10^{-5}, $M^{-1}s^{-1}$
TCP	10.2	8.5	13
TCA	6.3	7.6	5.3
TCS	17.5	11.3	5.5
O_2	4.5	6.9	-

3.3.2. Transient absorption spectroscopy

To further obtain a confirmation of the redox reaction and therefore of the formation of pollutant radical cations and reduced photocatalyst (NMQ$^{\bullet}$), laser flash photolysis experiments were performed. Initially, the reduced photocatalyst (NMQ$^{\bullet}$) was obtained upon laser flash excitation (355 nm) of a deaerated acetonitrile solution in the presence of a good electron donor as DABCO ($E_{DABCO^{+\bullet}/DABCO}$ = + 0.56 V *vs* SCE).[50] As expected, a weak broad signal centered at 400 nm was obtained, that was attributed to NMQ$^{\bullet}$, in agreement with the expected redox process (Fig. 6A).[28]

Next, NMQ^{+} was submitted to laser flash excitation in the presence of the contaminants (see Fig. 6B-D). No extra signals corresponding to the oxidized radical cations were found for TCP (see Fig. 5B) or TCS (see Fig. 6D) in the recorded spectral window (370-650 nm); yet the band centered at 400 nm due to the reduced photocatalyst acted as a confirmation of the redox reaction. The difference in the intensities of the bands due to NMQ$^{\bullet}$ obtained in the presence of TCP or TCS, could be correlated to the slower photodegration reaction in the case of TCS compared to TCP under deaerated irradiation (Fig. S5A). Nevertheless, in the case of TCA (Fig. 6C), in addition to the band due to NMQ$^{\bullet}$ a new strong band centered at 500 nm was obtained. This band was assigned to the TCA radical cation by comparison to the signal reported for thioanisole radical cation centered at 520 nm.[24]

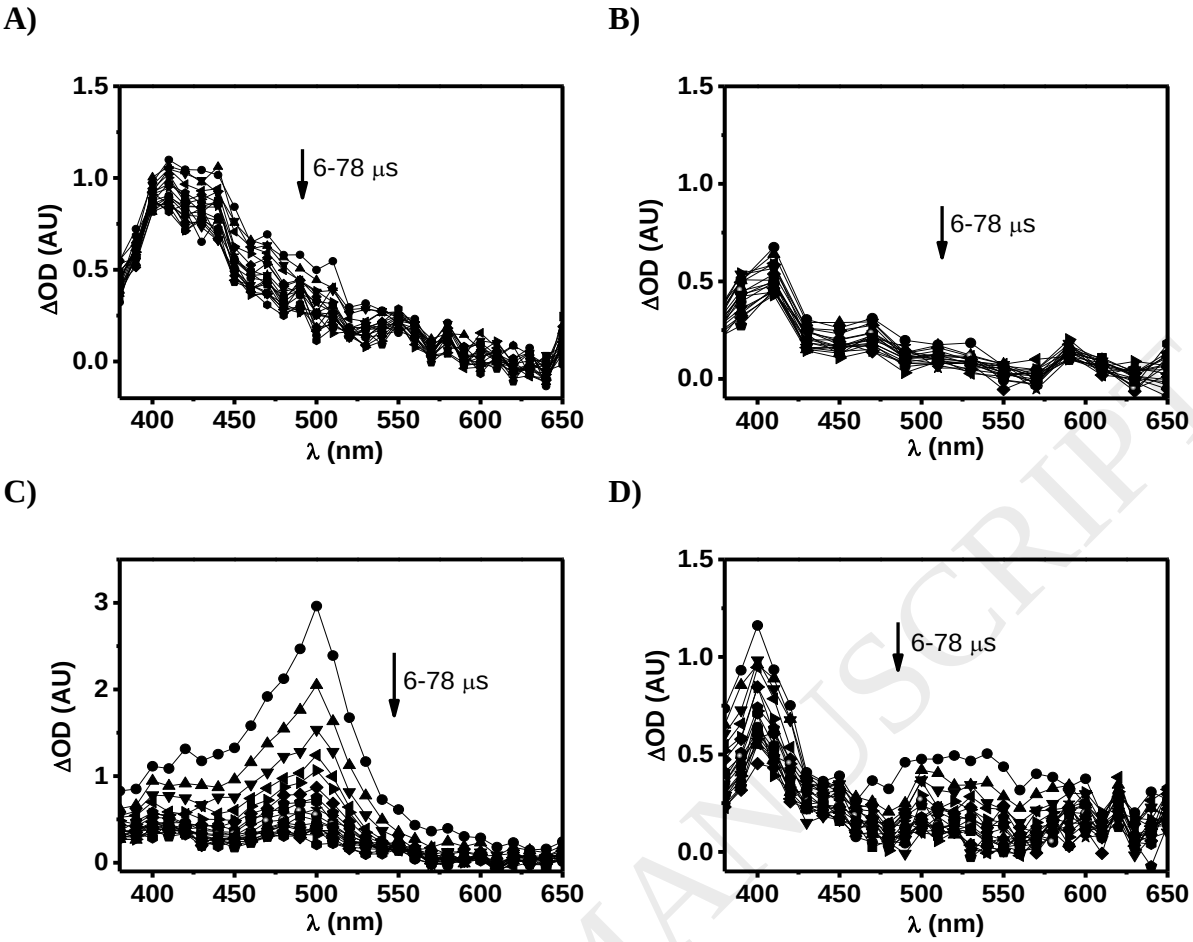

Figure 6

3.4. Mechanistic proposal

Scheme 1 shows the two main potential pathways investigated to explain the photodegradation of the selected contaminants.

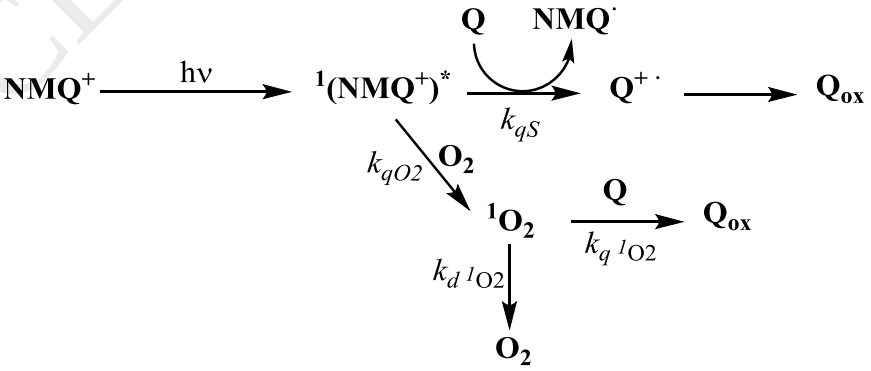

Scheme 1

As expected from the high redox potential of $^1(NMQ^+)^*$ and long singlet lifetime, quenching by the pollutants (k_{qS}) and by oxygen (k_{qO2}) is very efficient, with diffusion-controlled quenching constants (Table 2). This means that at ambient temperature in air-equilibrated water, where the concentration of O_2 is *ca.* 2.9×10^{-4} M,[50] if the pollutants are present at *ca.* 10^{-6}-10^{-5} M, formation of singlet oxygen accounts for more than 90% of $^1(NMQ^+)^*$ quenching, and less than 10% is due to direct electron transfer. However, quenching of $^1O_2$ by the contaminants is quite inefficient ($k_{q1_{O_2}}$ *ca.* 10^5-10^6 $M^{-1}s^{-1}$); thus at 10^{-6}-10^{-5} M pollutants concentration, quenching cannot compete with intrinsic deactivation ($k_q = 1/\tau$ *ca.* 10^6 s^{-1}). As a consequence, direct electron transfer (Type I) is the main operating pathway in the photodegradation of pollutants by NMQ^+ at concentrations in the micromolar range, in agreement with the observed photodegradation, independent on the presence of air. Since the quenching constants of $^1(NMQ^+)^*$ and $^1O_2$ by the pollutants are inherent to their nature and the concentration of O_2 in air-equilibrated water is only dependent on the temperature, the scenario can only be altered by modifying the contaminants' concentration. For instance, at higher concentrations, in the milimolar range, the electron transfer mechanism is responsible for more than 80% of $^1(NMQ^+)^*$ quenching; therefore Type I is again the main photodegradation pathway. On the other hand, with concentrations as low as 10^{-8} M, almost all the $^1(NMQ^+)^*$ quenching generates $^1O_2$, but quenching of $^1O_2$ by the pollutants at that concentration is completely inefficient compared to its intrinsic deactivation;[52] therefore photodegradation at such low concentrations is expected to be almost negligible.

4. Conclusions

Homogeneous photocatalytic degradation of highly chlorinated contaminants was efficiently achieved in the presence of NMQ^+. Photodegradation proceeded at similar rates, or even faster in the absence of air in the case of TCS. A high degree of detoxification was reached after 70 hours of irradiation, resulting in lower toxicity values than the ones shown by equivalent samples irradiated in the presence of TiO_2. Accordingly, fast-kinetics experiments demonstrated an efficient $^1(NMQ^+)^*$ quenching by the pollutants, with near diffusion-controlled rates, concomitant with the appearance of the reduced photocatalyst, that exhibits a transient absorption with a maximum at 400

nm. NMQ^+ is also able to generate singlet oxygen with high quantum yield. This singlet oxygen is also quenched by the selected contaminants at the typical $k_q = 10^5\text{-}10^6\ M^{-1}s^{-1}$. Nevertheless, kinetic analysis of the competitive photodegradation pathways indicates that electron transfer is the main photodegradation pathway independently of the pollutant concentration, being Type II mechanism negligible.

5. Acknowledgements

Financial support from Spanish Government (Grant SEV-2016-0683 and CTQ2015-69832-C4) and generous contribution from Generalitat Valenciana (Prometeo Program) are gratefully acknowledged. We also thank support from VLC/Campus. R. Martinez-Haya thanks financial support from Spanish Government (Grant SEV-2012-0267).

6. Figure captions

Figure 1. Chemical structures of the selected photocatalyst and contaminants.

Figure 2. Plot of the relative concentration of TCP (□), TCA (▲) and TCS (●) at C_0 = 3 x 10^{-5} M *vs* 350 nm irradiation time in the presence of NMQ^+ (3 x 10^{-7} M) under aerated atmosphere in aqueous media.

Figure 3. Plot of the relative concentration of TCP (□), TCA (▲) and TCS (●) at C_0 = 3 x 10^{-4} M *vs* 350 nm irradiation time in the presence of Zeolite Y-NMQ^+ (70 mg L^{-1}) under aerated atmosphere in aqueous media.

Figure 4. Evolution of % immobilization of *D. magna* bioassays conducted during the treatment of samples at several dilutions. Top: photomixture A (NMQ^+); Bottom: photomixture B (TiO_2). *Significant differences respect to treatment time ($p < 0.05$).

Figure 5. Left column: Steady-state and time-resolved (inset) $^1(NMQ^+)$* fluorescence quenching upon addition of increasing concentrations of pollutants ($[TCP]_{FINAL}$ = $[TCA]_{FINAL}$ = 5 x 10^{-3} M, $[TCS]_{FINAL}$ = 3 x 10^{-3} M) in ACN under N_2; λ_{exc} = 317 nm. Right column: Stern-Volmer plots obtained from the steady-state (dash) and time-resolved (solid) fluorescence quenching experiments.

Figure 6. Transient absorption spectra obtained upon laser flash excitation of NMQ^+ in deareated ACN (absorbance *ca.* 0.3 at 355 nm) recorded at different times after the laser pulse (6 – 78 μs) in the presence of (A) DABCO (5 x 10^{-2} M); (B) TCP (3 x 10^{-3} M); (C) TCA (3 x 10^{-3} M) and (D) TCS (3 x 10^{-3} M).

Scheme 1. Potential mechanistic pathways to explain photodegradation of the pollutants in the presence of NMQ^+.

7. Table legends

Table 1. EC_{50} values (95% confidence interval) determined for the photomixture compounds assayed separately.

Table 2. Rate constant values for the reaction between the pollutants and $^1(NMQ^+)$* obtained from the steady-state and time-resolved experiments (k_{qS}, $M^{-1}s^{-1}$), and for the reaction between $^1O_2$ and the pollutants ($k_{q^1O_2}$, $M^{-1}s^{-1}$).

8. References

[1] S. United Nations Educational, O. Cultural, UNESCO, (2006).
[2] H.K. Shon, S. Vigneswaran, S.A. Snyder, Crit. Rev. Env. Sci. Technol., 36 (2006) 327-374.
[3] S.J. Ren, Environ. Int., 30 (2004) 1151-1164.
[4] D. Rosner, G. Markowitz, Environ. Res., 120 (2013) 126-133.

[5] T. Openländer, Photochemical purification of water and air. Advanced oxidation processes: Principles, Reaction Mechanisms, Reactor concepts, Wiley, V. C. H., Weinheim, 2003.
[6] S. Malato, P. Fernandez-Ibanez, M.I. Maldonado, J. Blanco, W. Gernjak, Catal. Today, 147 (2009) 1-59.
[7] M.R. Hoffmann, S.T. Martin, W.Y. Choi, D.W. Bahnemann, Chem. Rev., 95 (1995) 69-96.
[8] J.C. Zhao, C.C. Chen, W.H. Ma, Top. Catal., 35 (2005) 269-278.
[9] E. Neyens, J. Baeyens, J. Hazard. Mater., 98 (2003) 33-50.
[10] M. Rodriguez, S. Malato, C. Pulgarin, S. Contreras, D. Curco, J. Gimenez, S. Esplugas, Sol. Energy, 79 (2005) 360-368.
[11] D. Ravelli, D. Dondi, M. Fagnoni, A. Albini, Chem. Soc. Rev., 38 (2009) 1999-2011.
[12] S. Rodriguez, A. Santos, A. Romero, Desalination, 280 (2011) 108-113.
[13] J.L. Wang, L.J. Xu, Crit. Rev. Env. Sci. Technol., 42 (2012) 251-325.
[14] J.J. Pignatello, E. Oliveros, A. MacKay, Crit. Rev. Env. Sci. Technol., 36 (2006) 1-84.
[15] S.K. Khetan, T.J. Collins, Chem. Rev., 107 (2007) 2319-2364.
[16] C. Tixier, H.P. Singer, S. Oellers, S.R. Müller, Environ. Sci. Technol., 37 (2003) 1061-1068.
[17] M.L. Marin, L. Santos-Juanes, A. Arques, A.M. Amat, M.A. Miranda, Chem. Rev., 112 (2012) 1710-1750.
[18] J. Gomis, A. Arques, A.M. Amat, M.L. Marin, M.A. Miranda, Appl. Catal. B, 123 (2012) 208-213.
[19] P. Miro, A. Arques, A.M. Amat, M.L. Marin, M.A. Miranda, Appl. Catal. B, 140 (2013) 412-418.
[20] D.C. Neckers, J. Photochem. Photobiol., A, 47 (1989) 1-29.
[21] J.S. Miller, Water Research, 39 (2005) 412-422.
[22] U.C. Yoon, S.L. Quillen, P.S. Mariano, R. Swanson, J.L. Stavinoha, E. Bay, J. Am. Chem. Soc., 105 (1983) 1204-1218.
[23] Y.A. Ilan, D. Meisel, G. Czapski, Isr. J. Chem., 12 (1974) 891-895.
[24] H. Yokoi, A. Hatta, K. Ishiguro, Y. Sawaki, J. Am. Chem. Soc., 120 (1998) 12728-12733.
[25] E. Baciocchi, T.D. Giacco, F. Elisei, M.F. Gerini, M. Guerra, A. Lapi, P. Liberali, J. Am. Chem. Soc., 125 (2003) 16444-16454.
[26] Y.K. Che, W.H. Ma, Y.J. Ren, C.C. Chen, X.Z. Zhang, J.C. Zhao, L. Zang, J. Phys. Chem. B, 109 (2005) 8270-8276.
[27] Y.K. Che, M.H. Ma, H.W. Ji, J.C. Zhao, L. Zang, J. Phys. Chem. B, 110 (2006) 2942-2948.
[28] E. Baciocchi, T. Del Giacco, M.F. Gerini, O. Lanzalunga, J. Phys. Chem. A, 110 (2006) 9940-9948.
[29] E. Baciocchi, T. Del Giacco, O. Lanzalunga, P. Mencarelli, B. Procacci, J. Org. Chem., 73 (2008) 5675-5682.
[30] E.L. Clennan, C. Liao, J. Am. Chem. Soc., 130 (2008) 4057-4068.
[31] P.F. Donovan, D.A. Conley, J. Chem. Eng. Data, 11 (1966) 614-&.
[32] Guidelines for Drinking-water Quality. Vol. 1: 3rd ed., WHO Library Cataloguing-in-Publication Data, Geneva, 2004.
[33] R. Martinez-Haya, M.H. Barecka, P. Miro, M.L. Marin, M.A. Miranda, Appl. Catal. B, 179 (2015) 433-438.
[34] A.E. Greyshock, P.J. Vikesland, Environ. Sci. Technol., 40 (2006) 2615-2622.

[35] F.M. Hamer, Journal of the Chemical Society (Resumed), (1939) 1008-1013.
[36] A. Arques, A.M. Amat, L. Santos-Juanes, R.F. Vercher, M.L. Marin, M.A. Miranda, Catal. Today, 144 (2009) 106-111.
[37] ISO, Water quality-determination of the inhibition of the mobility of Daphnia magna straus (Cladocera, Crustacea)-acute toxicity test, 1996, pp. pp. 6341.
[38] L. Xing, J. Sun, H. Liu, H. Yu, J. Environ. Monit., 14 (2012) 1677-1683.
[39] Y. Peng, Y. Luo, X.-P. Nie, W. Liao, Y.-F. Yang, G.-G. Ying, Ecotoxicology, 22 (2013) 1384-1394.
[40] D.B. Warheit, R.A. Hoke, C. Finlay, E.M. Donner, K.L. Reed, C.M. Sayes, Toxicol. Lett., 171 (2007) 99-110.
[41] X. Zhu, Y. Chang, Y. Chen, Chemosphere, 78 (2010) 209-215.
[42] G.P.S. Marcone, Á.C. Oliveira, G. Almeida, G.A. Umbuzeiro, W.F. Jardim, J. Hazard. Mater., 211-212 (2012) 436-442.
[43] W.H. Fan, M.M. Cui, H. Liu, C.A. Wang, Z.W. Shi, C. Tan, X.P. Yang, Environ. Pollut., 159 (2011) 729-734.
[44] A. Nel, T. Xia, L. Madler, N. Li, Science, 311 (2006) 622-627.
[45] K.T. Kim, S.J. Klaine, J. Cho, S.-H. Kim, S.D. Kim, Sci. Total Environ., 408 (2010) 2268-2272.
[46] M. Skocaj, M. Filipic, J. Petkovic, S. Novak, Radiology and Oncology, 45 (2011) 227-247.
[47] N.B. Hartmann, F. Von der Kammer, T. Hofmann, M. Baalousha, S. Ottofuelling, A. Baun, Toxicology, 269 (2010) 190-197.
[48] L. Clement, C. Hurel, N. Marmier, Chemosphere, 90 (2013) 1083-1090.
[49] P. Baveye, M. Laba, Environ. Health Perspect., 116 (2008) A152-A152.
[50] S.L. Murov, I. Carmichael, G.L. Hug, Handbook of Photochemistry, 2nd ed., Marcel Dekker, New York, 2009.
[51] C. Tournaire, S. Croux, M.-T. Maurette, I. Beck, M. Hocquaux, A.M. Braun, E. Oliveros, Journal of Photochemistry and Photobiology B: Biology, 19 (1993) 205-215.
[52] G.M. Rodriguez-Muñiz, J. Gomis, A. Arques, A.M. Amat, M.L. Marin, M.A. Miranda, Photochem. Photobiol., 90 (2014) 1467-1469.